Single-walled carbon-nanotube saturable absorber assisted Kerr-lens mode-locked Tm:$MgWO_4$ laser

Li Wang,[1] Weidong Chen,[1,2,*] Yongguang Zhao,[1] Yicheng Wang,[1,6] Zhongben Pan,[1] Haifeng Lin,[2] Ge Zhang,[2] Lizhen Zhang,[2] Zhoubin Lin,[2] Ji Eun Bae,[3] Tae Gwan Park,[3] Fabian Rotermund,[3] Pavel Loiko,[4] Xavier Mateos,[5] Mark Mero,[1] Uwe Griebner,[1] and Valentin Petrov[1]

[1]Max Born Institute for Nonlinear Optics and Short Pulse Spectroscopy, Max-Born-Str. 2a, 12489 Berlin, Germany
[2]Key Laboratory of Optoelectronic Materials Chemistry and Physics, Fujian Institute of Research on the Structure of Matter, Chinese Academy of Sciences, Fuzhou, 350002 Fujian, China
[3]Department of Physics, Korea Advanced Institute of Science and Technology (KAIST), 34141 Daejeon, Korea
[4]Centre de Recherche sur les Ions, les Matériaux et la Photonique (CIMAP), UMR 6252 CEA-CNRS-ENSICAEN, Université de Caen, 6 Boulevard du Maréchal Juin, 14050 Caen Cedex 4, France
[5]Universitat Rovira i Virgili (URV), Física i Cristal·lografia de Materials i Nanomaterials (FiCMA-FiCNA), 43007 Tarragona, Spain
[6]yicheng.wang@ruhr-uni-bochum.de
**Corresponding author: chenweidong@fjirsm.ac.cn*

Received XX Month XXXX; revised XX Month, XXXX; accepted XX Month XXXX; posted XX Month XXXX (Doc. ID XXXXX); published XX Month XXXX

We demonstrate sub-100 fs Kerr-lens mode-locking of a Tm:$MgWO_4$ laser emitting at ~2 μm assisted by a single-walled carbon nanotube saturable absorber. A maximum average output power of 100 mW is achieved with a pulse duration of 89 fs at a pulse repetition rate of ~86 MHz. The shortest pulse duration derived from frequency-resolved optical gating amounts to 76 fs at 2037 nm corresponding to nearly bandwidth-limited pulses. To the best of our knowledge, these are the shortest pulses generated from any Tm-doped tungstate crystal and the first report on saturable absorber assisted Kerr-lens mode-locking of a Tm laser at ~ 2 μm.

http://dx.doi.org/10.1364/OL.99.099999

A rapid progress in the generation of sub-100 fs ultrashort pulses from thulium (Tm^{3+}) solid-state lasers in the 2-μm spectral range started after the first demonstration of a Tm:$MgWO_4$ laser mode-locked (ML) by a graphene-based saturable absorber (SA) in 2017. Pulses as short as 86 fs at 2017 nm with an average output power of 39 mW were obtained directly from an ML oscillator [1]. Subsequently, slightly shorter (84 fs and 78 fs) pulses were generated using Tm-doped disordered garnet crystals Tm:CNNGG and Tm:CLNGG, and single-walled carbon-nanotubes based SAs (SWCNT-SAs) [2, 3]. After extra-cavity chirp compensation, pulses as short as 72 fs were obtained from a Kerr-lens ML Tm:Sc_2O_3 laser [4]. Sub-10 optical cycle pulse generation at ~2 μm was first demonstrated in 2018 based on a Tm:$(Lu,Sc)_2O_3$ "mixed" sesquioxide ceramic laser ML by a semiconductor saturable absorber mirror (SESAM) [5]. Further improvement in pulse shortening benefited from the usage of a SWCNT-SA in a ML Tm:$(Lu,Y)_2O_3$ "mixed" ceramic laser generating 57 fs pulses with an average output power of 63 mW [6]. The implementation of broadband chirped mirrors (CMs) exhibiting high reflectivity over 330 nm and almost flat group delay dispersion (GDD) over more than 300 nm for dispersion management together with selected host materials possessing broad and relatively smooth gain spectra in combination with natural emission above 2.0 μm [7] to overcome the problems related to water vapor absorption below 2.0 μm was instrumental for the above achievements.

Tungstates and molybdates represent a huge class of anisotropic crystalline materials with different crystallographic symmetries and offer polymorphism [8]. Most popular as laser hosts is the family of the monoclinic potassium rare-earth double tungstates since they contain optically passive ions that can be easily substituted by optically active trivalent lanthanides such as Tm^{3+}. In contrast to the cubic sesquioxides or garnets, the emission in such materials is naturally polarized. Tm:$KLu(WO_4)_2$ was employed in the first steady-state passively ML Tm-laser with a SWCNT-SA to generate ~10 ps pulses at ~1.95 μm [9]. The main challenge for achieving stable femtosecond ML operation with such crystals comes from the fact that the free-running emission wavelengths is well below 2.0 μm, in the range of strong and structured water vapor absorption. A spectrally selective element can be used to shift the central wavelength but this will narrow the spectrum. Thus, 386-fs pulses at 2030 nm were achieved from a

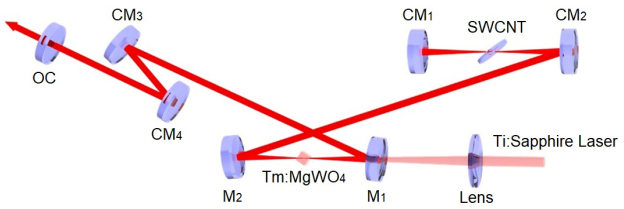

Fig. 1. Experimental arrangement of the ML Tm:$MgWO_4$ laser, Lens: pump focusing lens; M_1-M_2: concave dichroic mirrors; CM_1-CM_4, chirped mirrors; OC: output coupler.

SESAM ML Tm:$KY(WO_4)_2$ laser [10] and 141-fs pulses from a SWCNT-SA ML Tm:$KLu(WO_4)_2$ laser at 2037 nm [11].

Tm^{3+}:$MgWO_4$ (shortly Tm:MgW) is a representative of another family of monotungstate/monomolybdate crystals which exhibit the same monoclinic symmetry. It features (i) high thermal conductivity (~8.7 W/mK), which is beneficial for high power operation, (ii) extremely broad and smooth gain cross-section spectra supporting sub-100 fs pulses which is related to crystal field distortions when substituting the divalent Mg^{2+} host ions by Tm^{3+}, (iii) free-running emission wavelength above 2 µm, which overcomes the above mentioned problem of water vapor absorption causing ML instabilities in fs-pulse operation even without N_2 purging, and (iv) polarized absorption and emission, just as Tm:$KLu(WO_4)_2$, which offers more flexibility in pumping and spectral bandwidth utilization [12, 13]. The superior thermo-optical and spectroscopic properties motivated us to explore the potential of the Tm:MgW crystal for Kerr-lens ML (KLM) operation. To the best of our knowledge, so far there have been no reports on KLM operation based on a Tm-doped tungstate crystal operating at 2 µm. With the implementation of a SWCNT-SA for starting and stabilizing the KLM operation, in this work we achieve a pulse duration as short as 76 fs from the Tm:MgW oscillator. This result represents the shortest pulse duration ever achieved from any Tm-doped tungstate crystal and the first report on SA assisted KLM operation of a Tm laser at ~2 µm.

Laser operation was studied in an linear astigmatically compensated X-shaped cavity as shown in Fig. 1. The laser gain medium was an N_g-cut Tm:MgW crystal grown by the top-seeded solution growth method [14]. It had a measured Tm^{3+} concentration of 0.89 at.%, an aperture of 4 × 4 mm^2 and was 3-mm thick. The crystal was mounted in a water-cooled Cu holder (coolant temperature: 14 °C) and placed at Brewster's angle to select the highest gain of the N_m polarization, between two dichroic folding mirrors M_1 and M_2 (RoC = -100 mm). A second beam waist was created by using two curved chirped mirrors CM_1 (RoC = -50 mm) and CM_2 (RoC = - 150 mm). In continuous wave (CW) operation, with the SA removed, the other cavity arm contained only a plane-wedged output coupler (OC). The cavity mode inside the laser crystal was estimated by using the ABCD formalism giving a waist radius of 30 and 56 µm in the sagittal and tangential planes, respectively. A narrow-linewidth CW Ti:Sapphire laser tuned to 800 nm was employed as a pump source with polarization parallel to the N_m crystal axis. The pump beam was focused into the Tm:MgW crystal using a lens (focal length: f = 70 mm) yielding a radius of 30 µm. A maximum output power of 577 mW was obtained in the CW laser regime with 3% transmission of the OC at an absorbed pump power of 1.67 W corresponding to a slope efficiency of 35.5%. The experimentally measured single-pass pump absorption under lasing conditions

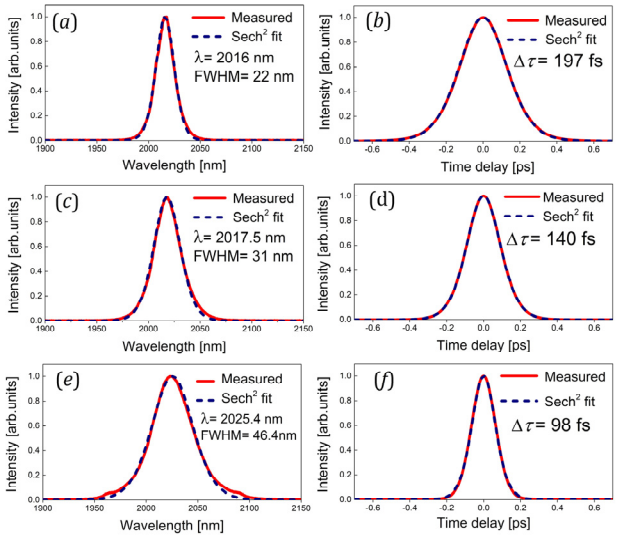

Fig. 2. Optical spectra (a, c and e) and the corresponding autocorrelation traces (b, d and f) of the ML Tm:MgW laser (T_{OC} = 1.5%).

slightly varied with the OC (0.5% - 5%) between 36% and 39%. A total round-trip resonator loss of δ = 0.85% (reabsorption losses excluded) was estimated with the Caird analysis by fitting the measured slope efficiency as a function of the OC reflectivity [15].

For ML operation, the SWCNT-SA was placed at Brewster's angle at the second beam waist between CM_1 and CM_2 for achieving soliton ML operation. The estimated radius of this second beam waist was 37 and 52 µm in the sagittal and tangential planes, respectively. The SWCNTs were fabricated by the arc-discharge method and were deposited on a 1 mm-thick uncoated quartz substrate acting as a transmission-type SA. Typical characteristics include a non-saturable loss of ~1%, a modulation depth of less than 0.5%, and a saturation fluence around 10 µJ/cm^2 [7, 16]. Two additional flat CMs, CM_3 and CM_4 were introduced in the other cavity arm for balancing the intracavity material dispersion and the induced self-phase modulation (SPM) during ML operation. All CMs used for intracavity dispersion management exhibited a GDD of -125 fs^2 per bounce.

In a first series of ML experiments the transition from SWCNT-SA ML to KLM is demonstrated. By employing a 1.5% OC, stable and self-starting fs ML operation was initiated by the SWCNT-SA at an absorbed pump power of 816 mW through its efficient bleaching. The 7 bounces of the laser beam on the CMs with a total round-trip GDD of -887 fs^2 ensured optimum performance with soliton-like pulses [see Fig. 2(a) and (b)]. The nearly perfect $sech^2$ fitting of both the measured ML spectrum and the autocorrelation trace yielded a pulse duration of 197 fs at 2016 nm with a spectral full width at half maximum (FWHM) of 22 nm and an average output power of 50 mW. In order to introduce an efficient soft-aperture Kerr-lens effect, we gradually enlarged the laser mode size inside the Tm:MgW crystal by varying the separation between the pump mirror M_1 and the folding mirror M_2 while keeping the same absorbed pump power [17]. A significant broadening of the ML spectra was observed when translating the folding mirror M_2 by several hundreds of micrometers away from the pump mirror M_1. In Fig. 2(a), (c) and (e), the FWHM of the ML spectra increased from 22 to 46.4 nm. The corresponding measured pulse duration decreased from 197 to 98 fs. The calculated time-bandwidth

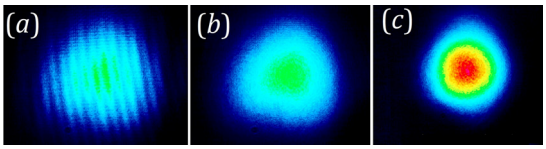

Fig. 3. Mode-locked Tm:MgW laser - transition of SWCNT-SA ML to KLM by changing the mirror separation M_1–M_2 (Toc = 1.5%). Far-field beam profiles: (a) CW; (b) SWCNTs-SA ML; and (c) KML.

product (TBP) remained almost unchanged, amounting to 0.32, 0.32 and 0.332 in the three cases. The central wavelength experienced a red-shift by ~9.4 nm, i.e., from 2016 to 2025.4 nm. Pulse shortening and the wavelength shift indicates that KLM became the dominant pulse shaping mechanism and the SWCNT-SA played the role as starter and stabilizer of the ML Tm:MgW laser. With the assistance of the SWCNT-SA, KLM operation of the Tm:MgW laser could be achieved without pushing the resonator to its stability edges to fulfill the requirement of a maximized self-amplitude modulation. The maximum average output power for KLM operation with 98 fs pulse duration was 72 mW at a pulse repetition rate of ~86 MHz. The corresponding on-axis intracavity laser intensity on the Tm:MgW crystal was calculated to be ~35.2 GW/cm^2.

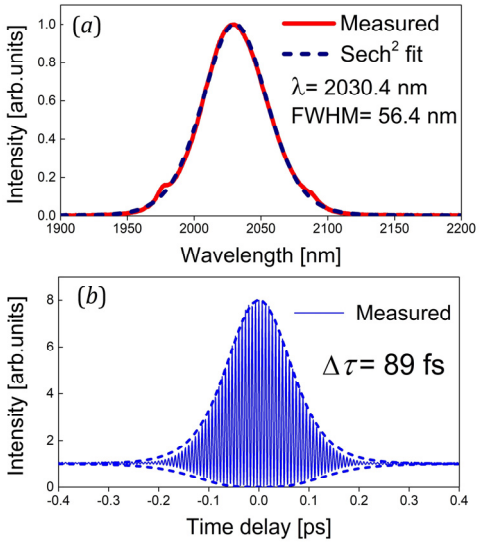

Fig. 4. (a) Optical spectrum and (b) interferometric autocorrelation trace of the mode-locked Tm:MgW laser with T_{oc} = 1.5%.

Soft-aperture KLM operation was further confirmed by monitoring the output beam profile, as shown in Fig. 3. A mid-IR Camera (DataRay, WinCamD) was placed at ~1.6 m away from the OC to measure the far-field beam profiles. In CW operation, the beam in the far-field had a diameter of 6.29 × 6.01 mm^2, as shown in Fig. 3(a). The strong interference fringes observed originated from reflections at the front and rear surfaces of a neutral density filter placed in front of the mid-IR camera. When mode-locking was initiated by the SWCNT-SA without soft-aperture Kerr-lens effect [cf. Fig. 2(a) and (b)], the interference fringes disappeared from the measured far-field beam profile due to the reduced coherence length which is shorter than the pulse duration, Fig. 3(b). The measured diameter of the beam in the far-field

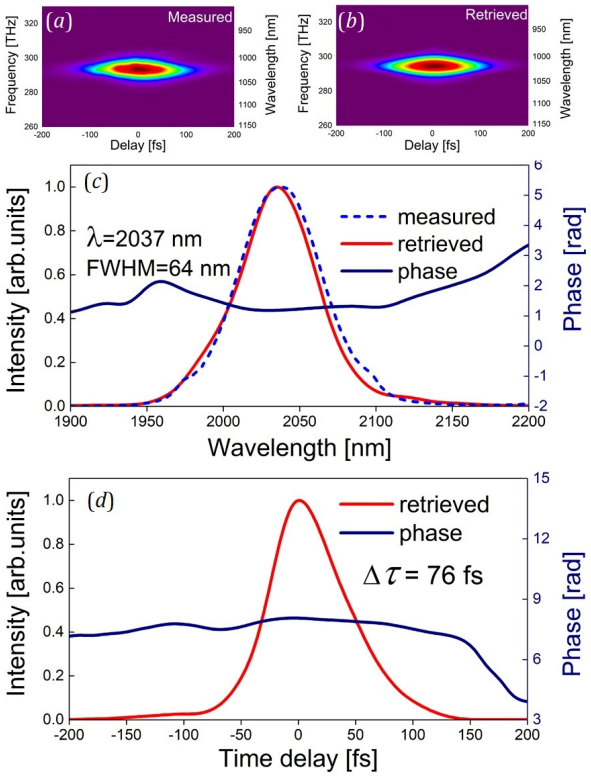

Fig. 5. (a) Measured and (b) retrieved SHG-FROG spectrogram of the Kerr-lens ML Tm:MgW laser (Toc = 0.5%). (c) Measured optical spectrum (dashed line) together with the retrieved one and the spectral phase. (d) Retrieved temporal intensity profile and the associated temporal phase.

amounted to 6.37 × 6.02 mm^2. The nearly identical sizes of the far-field beam profiles in CW and SWCNT-SA ML operation indicates a mostly absence of KLM. The transition to dominating soft-aperture KLM, i.e., strong self-focussing inside the Tm:MgW crystal with soft-aperture Kerr-lens effect [cf. Figs. 2(e) and (f)] is confirmed by shrinking of the diameter in the far-field beam profile to 4.96 × 4.67 mm^2, Fig. 3(c).

The second series of experiments aimed at the generation of the shortest pulses in the regime with dominating KLM. Scaling the absorbed pump power leads to shorter pulse. At an absorbed pump power of 1.12 W, the center wavelength of the KLM spectrum shifted to 2030.4 nm with a sech^2 fitted FWHM of 56.4 nm, as can be seen from Fig. 4(a). The measured interferometric autocorrelation trace gave a pulse duration of 89 fs, as shown in Fig. 4(b). The average output power increased to 100 mW at 86 MHz. The corresponding on-axis intracavity laser intensity on the Tm:MgW crystal increased to ~53.8 GW/cm^2.

The pulse duration could be further shortened by reducing the OC transmission to 0.5% at the expense of the average output power. Pulses as short as 80 fs were directly emitted from the self-starting KLM Tm:MgW oscillator with a measured spectral FWHM of 64.4 nm. The average output power in this case amounted to 35 mW for 881 mW of absorbed pump power. The slightly chirped pulses with a TBP of 0.372 were extra-cavity chirp compensated with a 3-mm-thick ZnS ceramic plate. The shortest pulses were characterization by second-harmonic generation (SHG) frequency-resolved optical gating (FROG) using a 1-mm-thick type-I $LiNbO_3$

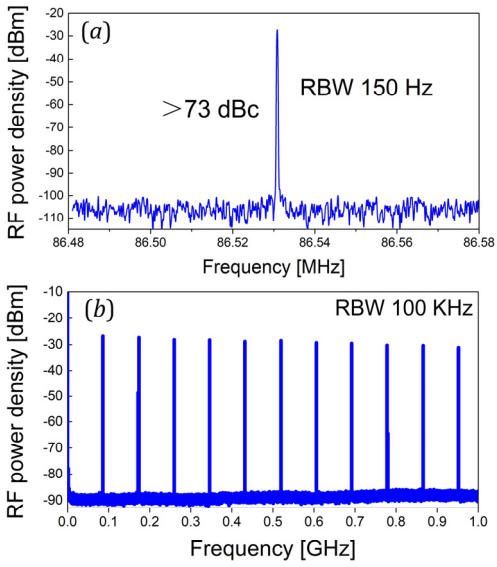

Fig. 6. Measured radio-frequency spectrum of the Kerr-lens mode-locked Tm:MgW laser: (a) Fundamental beat note at 86.5 MHz measured with a resolution bandwidth (RBW) of 150 Hz and (b) its harmonics on a 1-GHz span, measured with a RBW of 100 kHz.

crystal. The results are shown in Fig. 5. The measured SHG-FROG spectrogram was reconstructed with an error of 0.0054 on a 128 ×128 grid, Fig. 5(a) and (b). The independently measured ML spectrum agree well with the retrieved FROG spectrum yielding a spectral FWHM of 64 nm and a central wavelength of 2037 nm, as shown in Fig. 5(c). After extra-cavity chirp compensation, pulses as short as 76 fs were obtained, see the retrieved temporal profile in Fig. 5(d). The corresponding TBP of 0.354 indicates nearly bandwidth limited pulses.

The CWML pulse train was characterized by a radio-frequency analyzer. Figures 6 (a) and (b) show the fundamental beat note at ~86.5 MHz with a signal-to-noise ratio above 73 dBc and a1-GHz-wide span, both confirming the ultimate stability of the ML laser for the shortest pulse operation.

In conclusion, we realized saturable absorber assisted Kerr-lens mode-locking of a Tm solid-state laser at ~2 μm. With the help of a SWCNT-SA, Kerr-lens ML operation of the Tm:MgW laser does not require any critical cavity alignment or pushing the resonator to the stability limits, in contrast to pure Kerr-lens mode-locking. The maximum average output power of 100 mW was obtained for a pulse duration of 89 fs. The shortest pulse duration of 76 fs was be achieved after extra-cavity linear chirp compensation eliminating the residual chirp resulting from imperfect intracavity GDD compensation related t othe stepwise GDD management using chirp mirrors.

Funding. National Natural Science Foundation of China (61975208, 51761135115, 61575199, 61850410533, 52072351); Deutsche Forschungsgemeinschaft (PE 607/14-1); Laserlab-Europe (654148); Natural Science Foundation of Jiangsu Province (BK20190104); Sino-German Scientist Cooperation and Exchanges Mobility Programme (M-0040); China Academy of Engineering Physics (CAEP) (YZJJLX2018005); Fund of Key Laboratory of Optoelectronic Materials Chemistry and Physics; Chinese Academy of Sciences (2008DP173016); National Research Foundation of Korea (2020R1A4A2002828) and China Scholarship Council (CSC) (201704910363).

Acknowledgment. Y. Zhao acknowledges financial support from the Alexander von Humboldt Foundation through a Humboldt fellowship.

Disclosures. The authors declare no conflicts of interest

References

1. Y. Wang, W. Chen, M. Mero, L. Zhang, H. Lin, Z. Lin, G. Zhang, F. Rotermund, Y. J. Cho, P. Loiko, X. Mateos, U. Griebner, and V. Petrov, Opt. Lett. **42**, 3076 (2017).
2. Z. Pan, Y. Wang, Y. Zhao, H. Yuan, X. Dai, H. Cai, J. E. Bae, S. Y. Choi, F. Rotermund, X. Mateos, J. M. Serres, P. Loiko, U. Griebner, and V. Petrov, Photon. Res. **6**, 800 (2018).
3. Y. Wang, Y. Zhao, Z. Pan, J. E. Bae, S. Y. Choi, F. Rotermund, P. Loiko, J. M. Serres, X. Mateos, H. Yu, H. Zhang, M. Mero, U. Griebner, and V. Petrov, Opt. Lett. **43**, 4268 (2018).
4. A. Suzuki, C. Kränkel, and M. Tokurakawa, Appl. Phys. Express **13**, 052007 (2020).
5. Y. Wang, W. Jing, P. Loiko, Y. Zhao, H. Huang, X. Mateos, S. Suomalainen, A. Härkönen, M. Guina, U. Griebner, and V. Petrov, Opt. Express **26**, 10299 (2018).
6. Y. Zhao, L. Wang, Y. Wang, J. Zhang, P. Liu, X. Xu, Y. Liu, D. Shen, J. E. Bae, T. G. Park, F. Rotermund, X. Mateos, P. Loiko, Z. Wang, X. Xu, J. Xu, M. Mero, U. Griebner, V. Petrov, and W. Chen, Opt. Lett. **45**, 459 (2020).
7. V. Petrov, Y. Wang, W. Chen, Z. Pan, Y. Zhao, L. Wang, M. Mero, S. Y. Choi, F. Rotermund, W. B. Cho, W. Jing, H. Huang, H. Yuan, H. Cai, L. Zhang, Z. Lin, P. Loiko, X. Mateos, X. Xu, J. Xu, H. Yu, H. Zhang, S. Suomalainen, M. Guina, A. Härkönen, and U. Griebner, Proc. SPIE **11209**, 112094G (2019).
8. V. K. Trunov, V. A. Efremov, and Yu. A. Velikodnyi, **23**, Nauka, Leningrad (1986).
9. W. B. Cho, A. Schmidt, J. H. Yim, S. Y. Choi, S. Lee, F. Rotermund, U. Griebner, G. Steinmeyer, V. Petrov, X. Mateos, M. C. Pujol, J. J. Carvajal, M. Aguilo, and F. Diaz, Opt. Express **17**, 11007 (2009).
10. A. A. Lagatsky, S. Calvez, J. A. Gupta, V. E. Kisel, N. V. Kuleshov, C. T. A. Brown, M. D. Dawson, and W. Sibbett, Opt. Express **19**, 9995 (2011).
11. A. Schmidt, S. Y. Choi, D. I. Yeom, F. Rotermund, X. Mateos, M. Segura, F. Diaz, V. Petrov, and U. Griebner, Appl. Phys. Express **5** (2012).
12. P. Loiko, J. M. Serres, X. Mateos, M. Aguilo, F. Diaz, L. Z. Zhang, Z. B. Lin, H. F. Lin, G. Zhang, K. Yumashev, V. Petrov, U. Griebner, Y. C. Wang, S. Y. Choi, F. Rotermund, and W. D. Chen, Opt. Lett. **42**, 1177 (2017).
13. P. Loiko, Y. Wang, J. M. Serres, X. Mateos, M. Aguiló, F. Díaz, L. Zhang, Z. Lin, H. Lin, G. Zhang, E. Vilejshikova, E. Dunina, A. Kornienko, L. Fomicheva, V. Petrov, U. Griebner, and W. Chen, J. Alloys Compd. **763**, 581 (2018).
14. L. Zhang, H. Lin, G. Zhang, X. Mateos, J. M. Serres, M. Aguiló, F. Díaz, U. Griebner, V. Petrov, Y. Wang, P. Loiko, E. Vilejshikova, K. Yumashev, Z. Lin, and W. Chen, Opt. Express **25**, 3682 (2017).
15. J. A. Caird, S. A. Payne, P. R. Staber, A. J. Ramponi, L. L. Chase, and W. F. Krupke, IEEE J. Quantum Electron. **24**, 1077 (1988).
16. W. B. Cho, J. H. Yim, S. Y. Choi, S. Lee, A. Schmidt, G. Steinmeyer, U. Griebner, V. Petrov, D. I. Yeom, K. Kim, and F. Rotermund, Adv. Funct. Mater. **20**, 1937 (2010).
17. T. Brabec, C. Spielmann, P. F. Curley, and F. Krausz, Opt.s Lett. **17**, 1292 (1992).

References

1. Y. Wang, W. Chen, M. Mero, L. Zhang, H. Lin, Z. Lin, G. Zhang, F. Rotermund, Y. J. Cho, P. Loiko, X. Mateos, U. Griebner, and V. Petrov, "Sub-100 fs Tm:$MgWO_4$ laser at 2017 nm mode locked by a graphene saturable absorber," Optics Letters **42**, 3076-3079 (2017).
2. Z. Pan, Y. Wang, Y. Zhao, H. Yuan, X. Dai, H. Cai, J. E. Bae, S. Y. Choi, F. Rotermund, X. Mateos, J. M. Serres, P. Loiko, U. Griebner, and V. Petrov, "Generation of 84-fs pulses from a mode-locked Tm:CNNGG disordered garnet crystal laser," Photon. Res. **6**, 800-804 (2018).
3. Y. Wang, Y. Zhao, Z. Pan, J. E. Bae, S. Y. Choi, F. Rotermund, P. Loiko, J. M. Serres, X. Mateos, H. Yu, H. Zhang, M. Mero, U. Griebner, and V. Petrov, "78 fs SWCNT-SA mode-locked Tm:CLNGG disordered garnet crystal laser at 2017 nm," Optics Letters **43**, 4268-4271 (2018).
4. A. Suzuki, C. Kränkel, and M. Tokurakawa, "High quality-factor Kerr-lens mode-locked Tm:Sc_2O_3 single crystal laser with anomalous spectral broadening," Applied Physics Express **13**, 052007 (2020).
5. Y. Wang, W. Jing, P. Loiko, Y. Zhao, H. Huang, X. Mateos, S. Suomalainen, A. Härkönen, M. Guina, U. Griebner, and V. Petrov, "Sub-10 optical-cycle passively mode-locked Tm:$(Lu_{2/3}Sc_{1/3})_2O_3$ ceramic laser at 2 μm," Optics Express **26**, 10299-10304 (2018).
6. Y. Zhao, L. Wang, Y. Wang, J. Zhang, P. Liu, X. Xu, Y. Liu, D. Shen, J. E. Bae, T. G. Park, F. Rotermund, X. Mateos, P. Loiko, Z. Wang, X. Xu, J. Xu, M. Mero, U. Griebner, V. Petrov, and W. Chen, "SWCNT-SA mode-locked Tm:$LuYO_3$ ceramic laser delivering 8-optical-cycle pulses at 2.05 μm," Optics Letters **45**, 459-462 (2020).
7. V. Petrov, Y. Wang, W. Chen, Z. Pan, Y. Zhao, L. Wang, M. Mero, S. Y. Choi, F. Rotermund, W. B. Cho, W. Jing, H. Huang, H. Yuan, H. Cai, L. Zhang, Z. Lin, P. Loiko, X. Mateos, X. Xu, J. Xu, H. Yu, H. Zhang, S. Suomalainen, M. Guina, A. Härkönen, and U. Griebner, *Sub-100-fs bulk solid-state lasers near 2-micron* Proc. SPIE **11209**, 112094G (2019).
8. V. K. Trunov, V. A. Efremov, and Yu. A. Velikodnyi, Crystal Chemistry and Characteristics of Double Molybdates and Tungstates [in Russian], **23** Nauka, Leningrad (1986).
9. W. B. Cho, A. Schmidt, J. H. Yim, S. Y. Choi, S. Lee, F. Rotermund, U. Griebner, G. Steinmeyer, V. Petrov, X. Mateos, M. C. Pujol, J. J. Carvajal, M. Aguilo, and F. Diaz, "Passive mode-locking of a Tm-doped bulk laser near 2 μm using a carbon nanotube saturable absorber," Optics Express **17**, 11007-11012 (2009).
10. A. A. Lagatsky, S. Calvez, J. A. Gupta, V. E. Kisel, N. V. Kuleshov, C. T. A. Brown, M. D. Dawson, and W. Sibbett, "Broadly tunable femtosecond mode-locking in a Tm:KYW laser near 2 μm," Optics Express **19**, 9995-10000 (2011).
11. A. Schmidt, S. Y. Choi, D. I. Yeom, F. Rotermund, X. Mateos, M. Segura, F. Diaz, V. Petrov, and U. Griebner, "Femtosecond Pulses near 2 μm from a Tm:KLuW Laser Mode-Locked by a Single-Walled Carbon Nanotube Saturable Absorber," Applied Physics Express **5** (2012).
12. P. Loiko, J. M. Serres, X. Mateos, M. Aguilo, F. Diaz, L. Z. Zhang, Z. B. Lin, H. F. Lin, G. Zhang, K. Yumashev, V. Petrov, U. Griebner, Y. C. Wang, S. Y. Choi, F. Rotermund, and W. D. Chen, "Monoclinic Tm^{3+}:$MgWO_4$: a promising crystal for continuous-wave and passively Q-switched lasers at 2 μm," Optics Letters **42**, 1177-1180 (2017).
13. P. Loiko, Y. Wang, J. M. Serres, X. Mateos, M. Aguiló, F. Díaz, L. Zhang, Z. Lin, H. Lin, G. Zhang, E. Vilejshikova, E. Dunina, A. Kornienko, L. Fomicheva, V. Petrov, U. Griebner, and W. Chen, "Monoclinic Tm:$MgWO_4$ crystal: Crystal-field analysis, tunable and vibronic laser demonstration," Journal Alloys Compound **763**, 581-591 (2018).
14. L. Zhang, H. Lin, G. Zhang, X. Mateos, J. M. Serres, M. Aguiló, F. Díaz, U. Griebner, V. Petrov, Y. Wang, P. Loiko, E. Vilejshikova, K. Yumashev, Z. Lin, and W. Chen, "Crystal growth, optical spectroscopy and laser action of Tm^{3+}-doped monoclinic magnesium tungstate," Optics Express **25**, 3682-3693 (2017).
15. J. A. Caird, S. A. Payne, P. R. Staber, A. J. Ramponi, L. L. Chase, and W. F. Krupke, " Quantum electronic-properties of the Na3Ga2Li3F12:Cr^{3+} laser," IEEE Journal of Quantum Electronic **24**, 1077-1099 (1988).
16. W. B. Cho, J. H. Yim, S. Y. Choi, S. Lee, A. Schmidt, G. Steinmeyer, U. Griebner, V. Petrov, D. I. Yeom, K. Kim, and F. Rotermund, "Boosting the Nonlinear Optical Response of Carbon Nanotube Saturable Absorbers for Broadband Mode-Locking of Bulk Lasers," Advanced Functional Materials **20**, 1937-1943 (2010).
17. T. Brabec, C. Spielmann, P. F. Curley, and F. Krausz, "Kerr lens mode locking," Optics Letters **17**, 1292-1294 (1992).